



## Surface modification of composite polyamide reverse osmosis membrane by irradiated chitosan and TiO<sub>2</sub> nanoparticles

Hany M. Gayed<sup>a,\*</sup>, Faten Ismail Abou El Fadl<sup>a</sup>, Nabila A. Maziad<sup>a</sup>,  
Abdel Hameed M. El-Aassar<sup>b</sup>, M.S.A. Abdel-Mottaleb<sup>c</sup>

<sup>a</sup>Polymer Chemistry Department, National Center for Radiation Research and Technology (NCRRT), Egyptian Atomic Energy Authority, P.O. Box 29, Nasr city, Cairo, Egypt, email: hanygayed83@gmail.com (H.M. Gayed), fatenelramly555@yahoo.com (F.I.A. El Fadl), nabila\_maziad@yahoo.com (N.A. Maziad)

<sup>b</sup>Egyptian Desalination Research Center of Excellence (EDRC), Desert Research Center (DRC), Cairo, Egypt, email: hameed\_m50@hotmail.com (A.H.M. El-Assar)

<sup>c</sup>Faculty of Science, Ain Shams University, Cairo, Egypt, email: solar@photoenergy.org (M.S.A. Abdel Mottaleb)

Received 1 October 2018; Accepted 3 April 2019

### ABSTRACT

This study focuses on the surface modification of polyamide (PA) thin-film composite reverse osmosis (RO) membranes using irradiated chitosan/titanium dioxide (CS/TiO<sub>2</sub>) via Co<sup>60</sup> gamma ray. This modification was achieved through coating of a thin layer of gamma preirradiated chitosan onto the surface of commercial PA thin film composite membrane. The chitosan concentrations ranged from 0.2 to 0.6 wt% with different contents of TiO<sub>2</sub> nanoparticles irradiated at different doses. The surface morphology, surface hydrophilicity and membrane chemical composition before and after the modification were analyzed by scanning electron microscope (SEM), contact angle measurements and FT-IR spectroscopy. FT-IR spectroscopy of the synthesized membranes proved the incorporation of both CS and TiO<sub>2</sub> nanoparticles on the polyamide active layer. The performance of both neat and modified membranes for water desalination was evaluated. The results showed an improvement in the permeate flux of the membranes by increasing TiO<sub>2</sub> concentration up to 0.125 wt%, and then decreased at higher concentration of TiO<sub>2</sub>. Moreover, the salt rejection (%) increased at lower concentrations of TiO<sub>2</sub> and then decreased with increasing the TiO<sub>2</sub> content. Contact angle measurements revealed that the surface hydrophilicity of the membranes, improved by increasing TiO<sub>2</sub> concentration in chitosan solution.

**Keywords:** Surface modification; Desalination; Reverse osmosis; Thin-film composite; Gamma irradiation

### 1. Introduction

Desalination of sea water is the major leading way to compensate for the water shortage all over the world. Membranes innovation has been utilized for water treatment for over 45 years [1]. Many types of materials are available for the fabrication of membranes. These materials can generally be grouped into two principle bunches ceramic-based membrane and polymeric-based membrane. Each group

has its advantages over the other, but polymeric based membranes still promising in the field of water treatment [2]. The most important advantages of polymer-based membranes are flexible in design, cheapness, and can remove dissolved ions and organics more efficiently [3]. Nevertheless, they also have some disadvantages including high hydrophobicity, exposure to biofouling, low fluxes, and low mechanical strength. There are plenty of literatures on both ceramic and polymeric-based membranes [4–8]. In the most recent decades, reverse osmosis membrane technology has been broadly used in desalination and industrial water treatment [9,10].

\*Corresponding author.

RO is a pressure driven process that permits the lowering of water through a semipermeable membrane from a solution-diffusion mechanism [11,12]. Because high pressure is needed to stimulate water diffusion and subdue the osmotic pressure of the saline feed, the properties of RO membranes are quite important as factors that significantly determine the process performance and cost. At this time, most commercially ready RO membranes are thin film composite type, where a thin, aromatic polyamide barrier layer is formed on the microporous support layer, for example, polysulfone formed by interfacial polymerization process [13]. Thin film composite (TFC) aromatic polyamide reverse osmosis (RO) membranes with high permeability, ability and selectivity of working at low pressures have become extremely important in desalination of brackish and sea water [14], and in considerable areas of industrial separations due to their higher water flux and good rejection abilities [15]. However, the currently available polymeric membranes are often restricted because of the differentiation between the water flux and selectivity [16–19]. RO membranes with higher water flux, good salt rejection, and better fouling resistance are needed in order to reduce both the cost and the energy consumption required in producing a good purified product.

The purpose of this paper is to modify TFC membrane by both irradiated chitosan via  $\text{Co}^{60}$  gamma ray and  $\text{TiO}_2$  to overcome the challenges of limited water flux and salt rejection. The optimum preparation conditions of PA/CS and PA/CS/ $\text{TiO}_2$  membranes were investigated through studying the effect of different factors. The characterization of the modified membranes was achieved using different instruments such as SEM, contact angle measurement and FT-IR. Also, the evaluation of the prepared modified membranes was evaluated through measuring both permeate flux and

salt rejection (%) using NaCl feed solutions with different salinities at different applied pressures.

## 2. Experimental

### 2.1. Materials and reagents

Chitosan (Deacetylation 93%) was purchased from Oxford Lab Chem. Acetic acid was obtained from El Nasr pharmaceutical, chemical Co. Egypt. A spiral-wound commercial RO membrane element was purchased from the commercial thin-film composite polyamide DOW Company.

### 2.2. Preparation of modified membranes

Chitosan certain concentrations were prepared by dissolving specified weights in diluted (1%) acetic acid and stirred to form chitosan acetate solutions with various concentrations (0.1, 0.2, 0.4, and 0.6 wt%). The resultant viscous solutions were further stirred with different concentrations of  $\text{TiO}_2$  nanoparticles ranged from 0.125 to 1 wt% with respect to chitosan weight. The solutions were then poured into quick-fit tubes and the air was removed by bubbling nitrogen gas for at least 10 min. Irradiation of chitosan and chitosan/ $\text{TiO}_2$  solutions to the required doses was carried out at a dose rate of (2.5 kGy/h) in the  $\text{Co}^{60}$  gamma cell in National Center for Radiation Research and Technology, Egyptian Atomic Energy Authority. The surface modification of TFC membranes was achieved using the irradiated solutions via the rocker table for 30 min to obtain a uniform thickness layer. After that, the membrane was annealed for 15 min at  $70^\circ\text{C}$ . The suggested reaction pathway is illustrated as shown in Fig. 1.

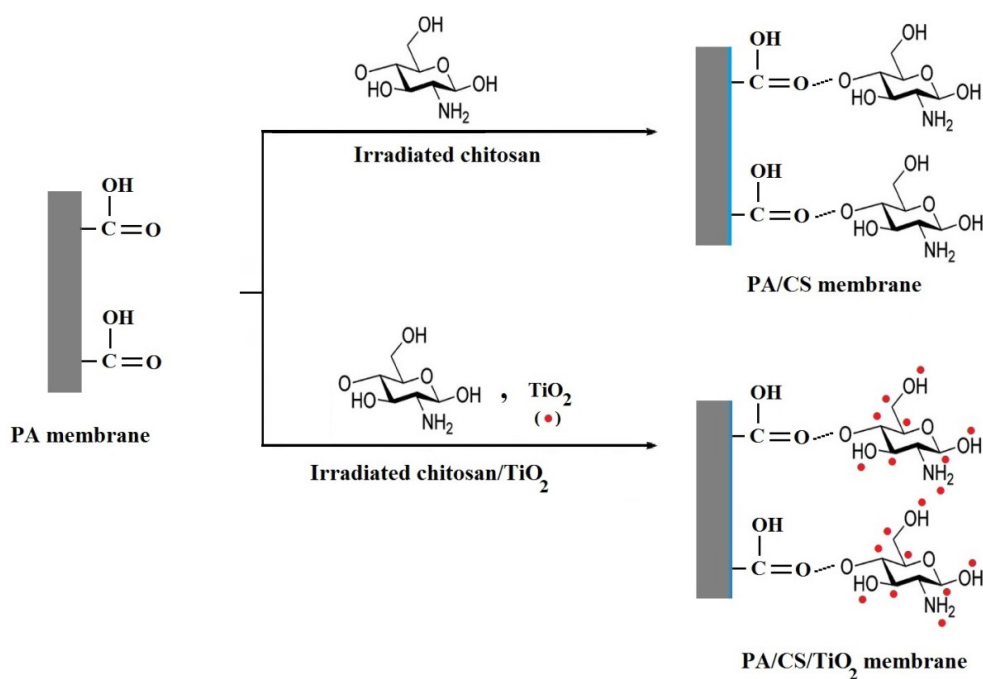


Fig 1. The schematic diagram of surface modification of PA membrane by chitosan and chitosan/ $\text{TiO}_2$ .

### 2.3. Characterization of modified membranes

#### 2.3.1. FTIR analysis

Fourier transform infrared spectroscopy (FTIR) was employed for analysis the surface composition of the neat and modified TFC polyamide RO membranes. The membrane test samples for FTIR analysis were dried at 25°C under vacuum before characterization. FTIR spectra were recorded on a Nicolet Aratar 370 FTIR spectrometer with a ZnSe crystal as the internal reflection element with an angle of incidence of 45°.

#### 2.3.2. SEM analysis

Scanning electron microscopy of the membrane surface was examined with JEOL JSM-5400 scanning electron microscopy (Japan), available at NCRRT.

#### 2.3.3. The x-ray diffraction (XRD)

The XRD analysis was performed using XD-DI Series, Shimadzu apparatus using nickel-filtered and Cu-K target. Available in NCRRT.

#### 2.3.4. Thermal gravimetric analysis (TGA)

Thermal gravimetric analyzer Shimadzu TGA arrangement of sort TGA-50 was utilized for this investigation. The temperature run was from encompassing to 600°C at a warming rate of 10°C/min under nitrogen air at stream rate 20 ml/min. The essential TGA thermo-grams were utilized to decide the rate of warm deterioration response.

#### 2.3.5. Contact angle measurements

The hydrophilicity of the membranes was determined by the contact angle measured using a DSA100 contact angle analyzer (KRUSS, Germany). All modified membrane samples and neat membrane were dried to remove the water in the TFC membranes and tested at least three measurements.

### 2.4. Evaluation of membrane performance:

The reverse osmosis performance of different types membranes included polyamide/chitosan (PA/CS) and polyamide/chitosan//TiO<sub>2</sub> (PA/CS/TiO<sub>2</sub>) membranes was evaluated through measuring both reverse osmosis parameters; permeate flux (L/m<sup>2</sup>·h) and salt rejection (%). Permeate flux and salt rejection were measured using cross-flow filtration using different aqueous feed solutions containing different concentrations (ppm) of NaCl at 25°C. The permeate flux and salt rejection were evaluated from the cross-flow experiment M20. The permeation flux ( $J$ ) through a membrane area ( $A$ ) was calculated as the volume ( $Q$ ) collected during a time period  $\Delta t$  [20] from Eq. (1).

$$J = Q/A \cdot \Delta t \quad (1)$$

Also, the salt rejection ( $R_s$  %) was calculated by measuring the electric conductivity of both feed and permeate solutions using JENWAY Laboratory bench conductivity meter (4510) and calculated as follows using Eq. (2):

$$R_s \% = (C_f - C_p/C_f) \times 100 \quad (2)$$

where  $C_f$  and  $C_p$  are the concentrations of the feed and permeate water, respectively.

## 3. Results and discussion

### 3.1. Characterization of neat and modified polyamide membranes

#### 3.1.1. FTIR analysis

In this work FTIR was used to assess chemical changes across the PA surface after surface modification through coating with chitosan and chitosan/TiO<sub>2</sub> mixture. Also, FTIR spectroscopy can give an advantage and successful approach to decide the composition of outmost parts in a thin film composite RO membrane where the PA membrane chemical structure is illustrated in Fig. 2.

The changes in chemical structure due to the modification process through coating with chitosan and chitosan/

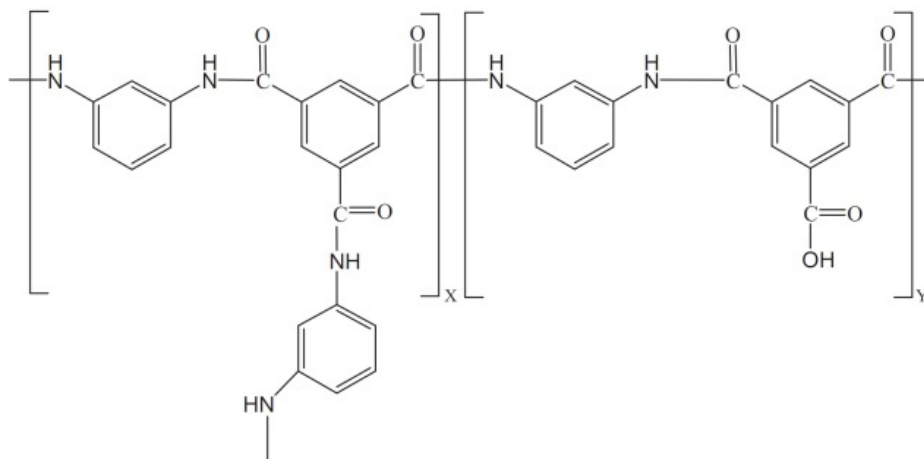


Fig. 2. The polyamide RO barrier layer derived structure.

TiO<sub>2</sub> mixtures were measured by FTIR and the results are shown in Fig. 3. The bonding structure of the polyamide active skin layer and the polysulfone supporting layer are shown in the range of 1750–750 cm<sup>-1</sup>. Bands that are related to polyamides can be found in the (range from 2800 to 3500) cm<sup>-1</sup> that represent C-O, C-N stretching, C-C-N deformation, vibration (amide I), N-H deformation vibration and C=C stretching vibration of aromatic amide, N-H bending, N-C stretching vibration of a -CO-NH- group (amide II), and OH group respectively [21,22]. It is clearly appeared from Fig. 3, the effect of coating with chitosan and TiO<sub>2</sub> on the characteristic bands of PA membrane where the intensity of bands attributed to certain functional groups as amid II and OH appeared in the range (2800 to 3500), increased as shown in Table 1. These results may due to the formation of hydrogen bonding and also the physical interaction between chitosan, TiO<sub>2</sub> and PA membrane. Also, it is important to mention here the appearance of a new band at nearly 940 cm<sup>-1</sup> which is attributed to the O-Ti-O and this consequently proves the presence of TiO<sub>2</sub>. In addition to the results showed in Table 1, the characteristic peaks of Fig.

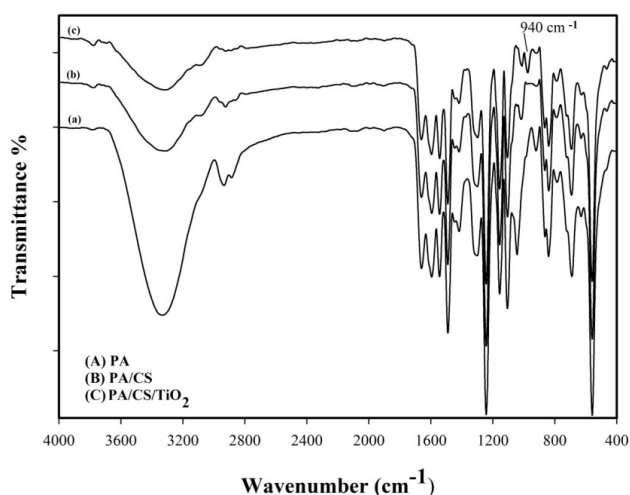


Fig. 3. FTIR spectra of PA(a), PA/CS(b), and PA/CS/TiO<sub>2</sub>(c) RO membranes.

Table 1

The intensities of various functional groups of PA, PA/CS/ and PA/CS/TiO<sub>2</sub> as illustrated in the FTIR spectra

Assignment	PA		PA/CS		PA/CS/TiO <sub>2</sub>	
	Wavenumber (cm <sup>-1</sup> )	Transmittance (%)	Wavenumber (cm <sup>-1</sup> )	Transmittance (%)	Wavenumber (cm <sup>-1</sup> )	Transmittance (%)
O-H	3367	75.26	3319.65	90.67	3302.3	92.89
HN-C=O amide	1666.36	81.55	1676	85.04	1677.93	86.07
C=O group	1596.8	79.78	1620.07	82.95	1627.79	85.06
Polysulfone group	1548.71	80.61	1577.6	82.37	1577.64	82.98
Aromatic ether stretching	1243.98	60.66	1249.77	64.39	1251	66.5
C-O stretching	1108.98	76.03	1116.69	81.4	1141.76	83.32
C-O stretching	1047.26	83.25	999.04	94.45	995.18	95.37
CH <sub>2</sub> Rock	922.33	96.71	915.6	99.73	920.13	97.82
O-Ti-O	0	0	0	0	940	98.02

3c is shifted to higher wavenumber, the wide peak at 3350 cm<sup>-1</sup>, corresponding to the stretching vibration of hydroxyl, amino and amide groups, moved conspicuously to higher wavenumbers 3300 cm<sup>-1</sup>, and became broader with higher intensity, which confirm the formation of nanocomposites of chitosan and TiO<sub>2</sub>.

### 3.1.2. Morphological study of membrane and modified membrane

SEM is a powerful technique for studying the morphology of the different membranes and also it gives a reasonable image of the change in the surface morphology as a result of modifications. Fig. 4 shows the cross-sectional SEM images of: the commercial polyamide reverse osmosis membrane, the modified membrane by irradiated chitosan, and the modified membrane by chitosan/TiO<sub>2</sub>. The SEM image of the commercial polyamide membrane, shown in (Fig. 4a), articulates a smooth surface with a small, intense of irritates and hills all over the surface and cross-sectional area. (Fig. 4b) shows the treatment of the membrane with chitosan under exposure to gamma radiation resulted in a great change in the morphology and became completely different where it appeared rough, spongy like and so jagged full of pores. Incorporation of TiO<sub>2</sub> into the coated membrane with chitosan as shown in (Fig. 4c), significantly altered the surface morphology in case of membrane coated with chitosan only, except dimensioning the size of pores and look like a compact sponge.

### 3.1.3. X-Ray diffraction of polyamide membrane and modified membrane

The XRD pattern of the polyamide membrane and the modified membrane with chitosan/TiO<sub>2</sub> mixture is illustrated in Fig. 5. It is well known that chitosan typical beaks appeared at 10.67° and 21.8° as confirmed in the literature [23] and also the TiO<sub>2</sub> is characterized by its peaks at 2-theta 25.1°, 37.2°, 48.49°, 54.2°, and 68.90° were assigned to the (100), (101), (110), (103), and (112) planes of distorted octahedral titanium dioxide can be indexed to the anatase TiO<sub>2</sub> with high crystallinity [24]. On the other hand, examining

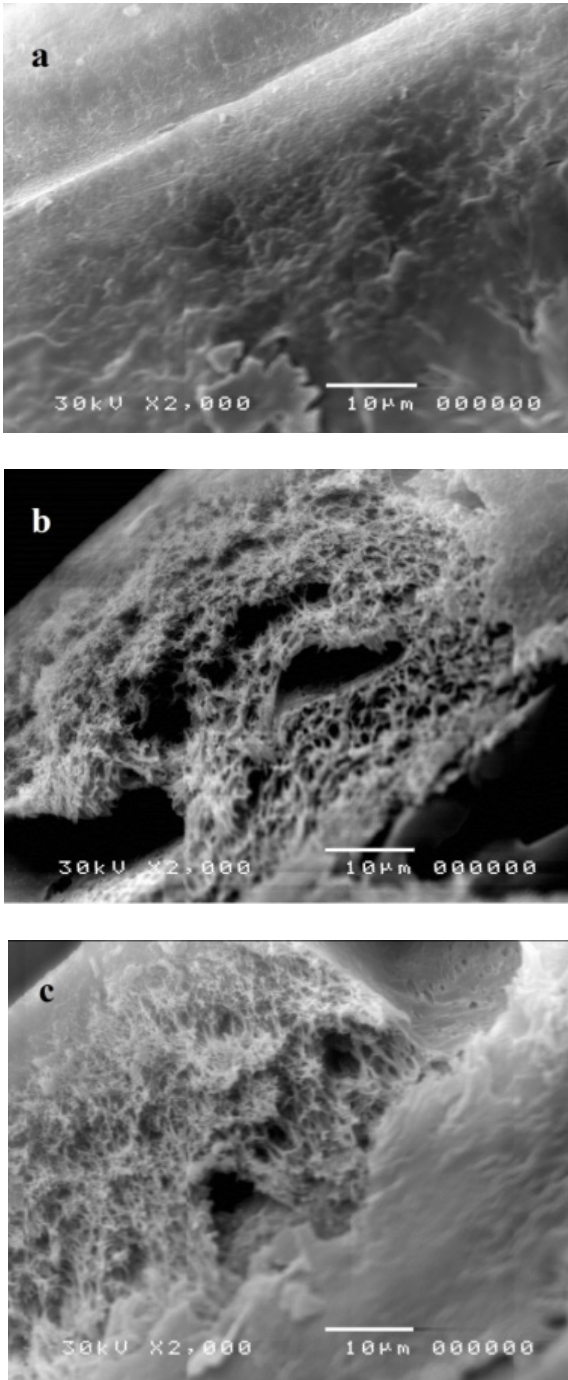


Fig. 4. Cross-sectional SEM micrographs of the commercial polyamide membrane (a), the modified membrane by chitosan (b) and chitosan/TiO<sub>2</sub> (c).

the XRD pattern of the polyamide membrane, shown in Fig. 5, revealed that the PA active layer of TFC membrane is characterized by the presence of three semi-crystalline peaks at  $2\theta$  of 17.85, 22.75 and 25.8°. By comparing neat membrane and modified membrane, it was found that the main characteristic peaks of PA/CS/TiO<sub>2</sub> membrane has broadened and shifted to nearly 25.42° due to the presence of TiO<sub>2</sub> nanoparticles [23]. The broad peaks represent small particle size and

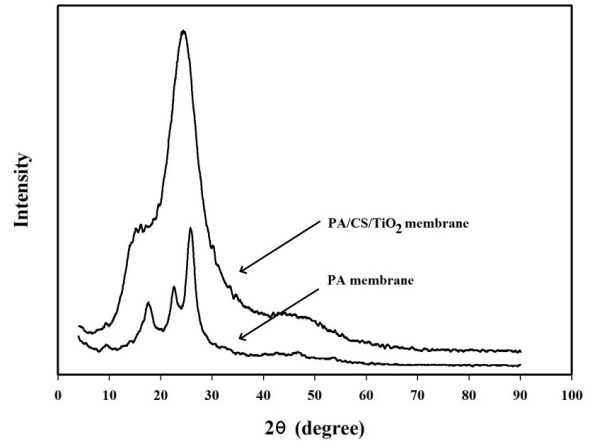


Fig. 5. XRD pattern of PA and PA/CS/TiO<sub>2</sub> membranes.

the material became amorphous due to the strong interaction between the membrane and the coating mixture. The main peak of TiO<sub>2</sub> still exists at 25.37°, which is in agreement with standard diffraction of TiO<sub>2</sub> ICDS #24276. It indicates that the modification of the polyamide membrane with chitosan and TiO<sub>2</sub> did not change the phase of TiO<sub>2</sub> but it decreased the particle size and the crystallinity which was shown by broad peaks [25].

#### 3.1.4. Thermal properties of polyamide membrane and modified membrane

Also, the thermal performance of the fabricated polymer is an important property to evaluate the modifying effects on the degradation behavior of polyamide membrane. (TGA) as a common thermal analysis method was used to study the thermal stability of PA, PA/CS, and PA/CS/TiO<sub>2</sub> membranes and the results illustrated in Fig. 6. It can be observed that for all PA, PA/CS, and PA/CS/TiO<sub>2</sub> membranes the thermal degradation took place through one thermal stage start from 45 to 380°C, but in case of treated membrane with both chitosan and CS/TiO<sub>2</sub> mixture a small thermal stage appeared in the temperature range 400–450°C due to the degradation of chitosan. Also, it appears from the thermal degradation of the PA, PA/CS, and PA/CS/TiO<sub>2</sub> the weight residues of them were 25%, 16%, and 14% respectively. According to the derivative of TGA curves, illustrated in Fig. 6.

For PA, PA/CS, and PA/CS/TiO<sub>2</sub> composite membranes, it showed the  $T_{max}$  appeared at 432, 433, and 430°C, respectively. The results obtained in Fig. 6, and Table 2 proves that the main degradation was in the PA chains and the coating with chitosan and TiO<sub>2</sub> slightly affect the thermal degradation of the PA composite membranes. These results are in agreement with the XRD results where the coating with chitosan and TiO<sub>2</sub> increased the amorphous nature of the polyamide membrane and consequently decreases the thermal properties.

#### 3.2. Membrane performance

The main target of modification of the commercial RO membranes is to increase the salt rejection and water flux,

which are the most important parameters that the authors work on them and also main reasons behind the intense development in this area.

### 3.2.1. Effect of chitosan concentration

Chitosan is a natural polymer with unique properties one of them is its antibacterial property which is useful to decrease the fouling effect on the prolonged use of RO membranes. In this study, various concentrations of chitosan were used for coating of PA membrane. The water flux and salt rejection are studied in Fig. 7 (a and b). It is noticed from the figure, that the salinity of the medium has a great and a sensitive effect on the water flux of the membranes under investigation with and without modification. As it is clearly appeared, the membranes behave differently before and after modification where the water flux of unmodified membrane decreased with increasing salinity (from 2000 to 20000 ppm) from nearly 60% to 33% with increasing the chitosan concentration up to 0.2% the water flux increased in case of high salinity concentrations (10000, 20000 ppm) then with further increase in chitosan concentration up to 0.6% the water flux decrease. While in case of low salinity concentration (2000 ppm) the water flux decreased, then increased as chitosan concentration increased to 0.6 wt% from 25% to 40%. On the other hand, the water flux of membranes at salinity concentration 5000 ppm, decreased at all chitosan concentration ranges.

To the extent the pervasion flux is concerned, the accompanying two contradicting impacts can be considered. From one viewpoint, the chitosan layer kept on the PA film sur-

face gives extra mass transfer resistance, in this way reducing the permeation flux. Then again, cationic chitosanium is more hydrophilic than PA and the improved hydrophilicity of the skin layer supports the sorption of water molecules. In weakened chitosan arrangements, the macromolecules are all around extended and scattered, and in this manner these atoms frames a generally free layer on the PA film substrate. As the chitosan fixation builds, the chitosan chains will be less extended because of the charge adjust of counter-ions [26]. On the other hand, by studying the effect of chitosan concentrations on the salt rejection ability of the investigated membranes, it is appeared to have stable trend as illustrated in Fig. 7b. Where at all chitosan concentrations

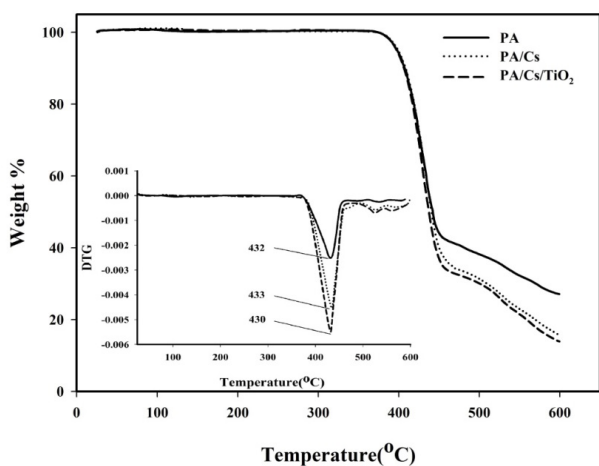


Fig. 6. The thermal behavior of PA, PA/CS, and PA/CS/TiO<sub>2</sub>.

Table 2

Weight loss (%) of PA, PA/CS, and PA/CS/TiO<sub>2</sub> membranes at various temperatures

Membrane	Weight loss (%) at different temperature									
	200°C	250°C	300°C	350°C	400°C	450°C	500°C	550°C	600°C	
PA	0.09	0.21	0.3	0.5	6.62	56.33	62.11	67.99	75.08	
PA/CS	0.1	0.15	0.28	0.6	5.87	60.06	68.86	77.15	84.02	
PA/CS/TiO <sub>2</sub>	0.15	0.18	0.2	0.3	7.12	63.43	70.11	78.65	86.18	

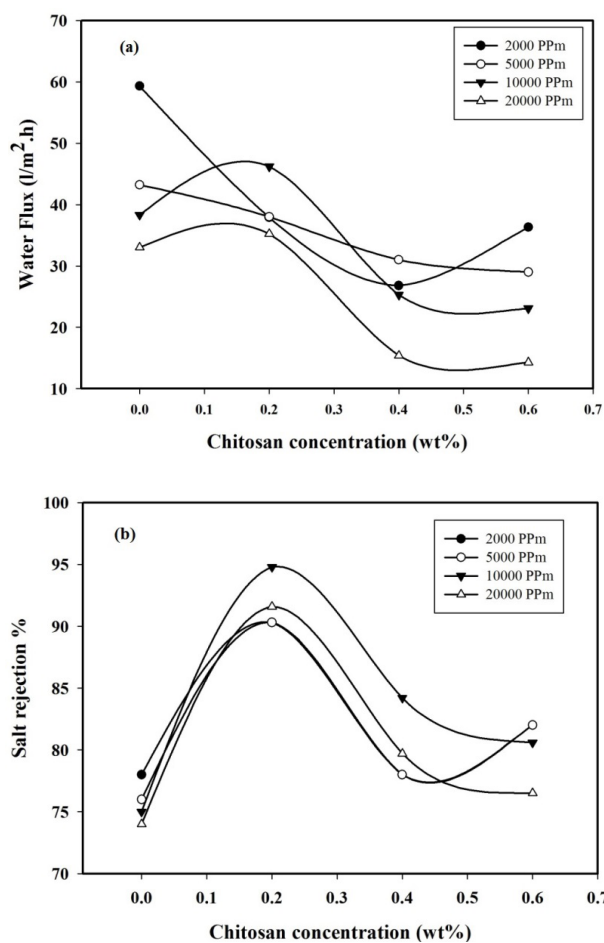


Fig. 7. The effect of chitosan concentration on the water flux- (a) and salt rejection (b) of polyamide and polyamide/chitosan membranes testing at 20 bar.

(0.2–0.6 wt.%) the salt rejection increased dramatically from nearly 73 to 95% with increasing chitosan concentration up to 0.2 wt% then decreased again. The change in the salt rejection can be credited to the expanded size sieving impact due to the thick and more reduced pressing of chitosan on the membrane surface. That may attribute to the fact that increasing the polymer content may cause the closing of the PA membrane pores and as a result its performance. It is clear from Fig. 7b, that the most suitable chitosan concentration is 0.2 wt% for water flux and salt rejection which reached nearly 50 (L/m<sup>2</sup>·h) water flux at salinity concentration of 10000 ppm. While salt rejection percent reached to 95.5%, at salinity concentration of 10000 ppm.

### 3.2.2. Effect of applied pressure

Pressure is another important factor that affects the membrane performance and it is essential to study its effect. By examining the PA membrane for its water flux under exposure to various pressures expressed in Pascal as shown in Fig. 8, and also, at various salinity concentrations (2000, 5000, 10000, and 20000), it is noticed that the water flux increased with increasing the applied pressure from 10 to 25 bar. The maximum water flux was nearly 47 L/m<sup>2</sup>·h under pressure of 25 bar and salinity of 10000 ppm. Considering

the results of salt rejection under various pressure forces, the behavior of the membrane was a little bit different and it did not follow a stable trend as in case of water flux as shown in Fig. 8b.

### 3.2.3. Effect of radiation doses

As the polymers and chemical materials affected when exposed to gamma radiation, especially natural polymers like chitosan, it is essential to study the effect of radiation on the membrane performance under the same conditions. Fig. 9 illustrates the effect of exposure to gamma radiation on the water flux and salt rejection, it is clear from the figures that the water flux and salt rejection of the membranes follow nearly the same stable trend under the effect of radiation and the highest water flux and salt ejection were at a dose of 15 kGy and salinity 10000 ppm. By increasing of irradiation doses the water flux and salt rejection decreasing due to the chitosan degradation.

### 3.2.4. Effect of TiO<sub>2</sub> concentration

The effect of TiO<sub>2</sub> concentration on the performance of membranes expressed in the water flux and salt rejection

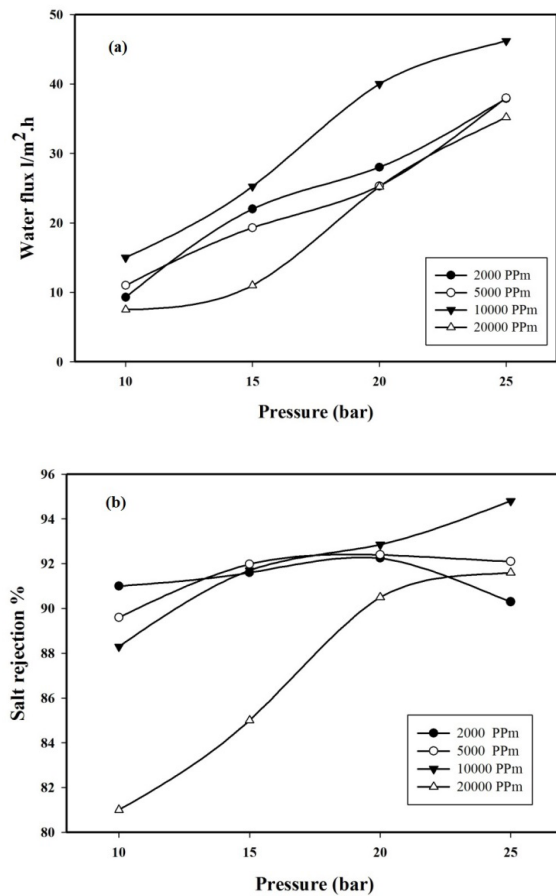


Fig. 8. The effect of pressure on the water flux (a) and salt rejection (b) of polyamide/chitosan membrane testing at chitosan concentration 0.2% at different salinities.

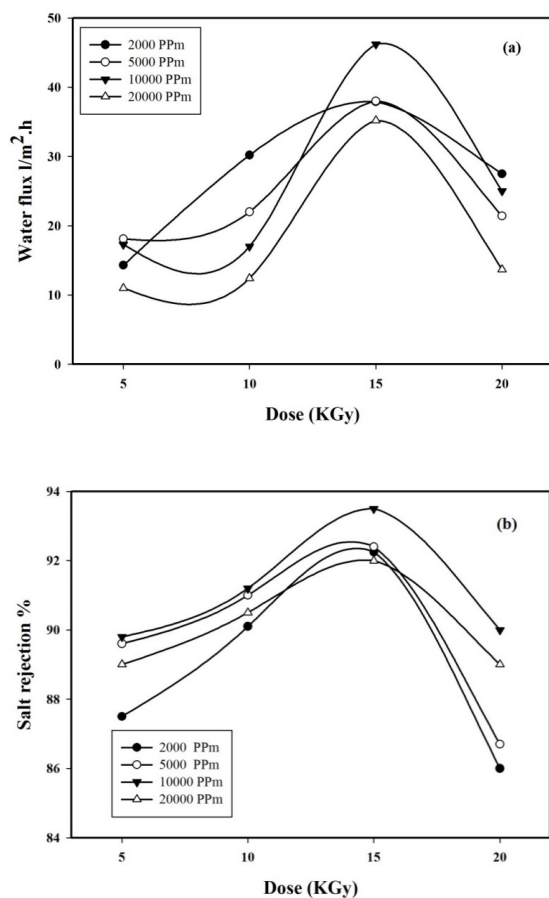


Fig. 9. The effect of irradiation dose on the water flux (a) and salt rejection (b) of Polyamide/chitosan membrane at chitosan concentration 0.2% testing at 20 bar.

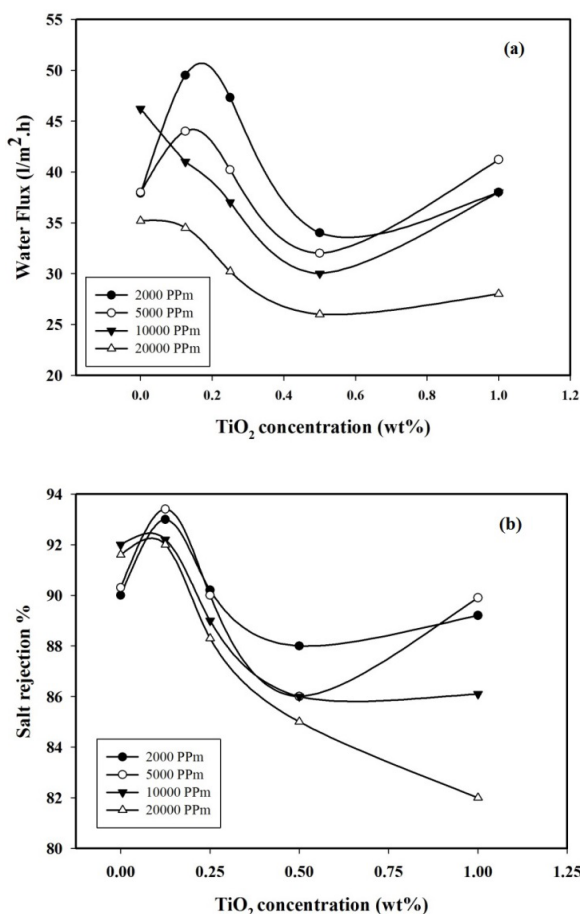


Fig. 10. The effect of TiO<sub>2</sub> concentration on the water flux (a) and salt rejection (b) of PA/CS/TiO<sub>2</sub> membrane testing at 20 bar with chitosan concentration 0.2% at irradiation dose 15 KGy.

is shown in Fig. 10. In this study, it needs only a very small concentration to achieve nearly 94% of a salt rejection and nearly 50 L/m<sup>2</sup>·h of a water flux. These results may be because of at very low concentration on TiO<sub>2</sub> nanoparticles the disparity is high and so it spread homogeneously all over the membrane where no agglomeration took place as depicted by SEM micrographs. Also, it is noticed that the performance of the investigated membranes after incorporation of TiO<sub>2</sub> nanoparticles was high at low salinity concentration (2000 and 5000 ppm).

### 3.3. Hydrophilicity of the membranes

The contact angle examination is one of the basic parameters for determining membrane surface charges and hydrophilic/hydrophobic properties which have a great influence on membrane both water permeability and susceptibility for fouling. While as contact angle becomes lower this means that the membrane surface turns to be more hydrophilic as the water particles have a greater tendency to wet the surface layer. This, in turn, raises the membrane water flux [27].

Contact angles ( $\theta$ ) were measured to determine the change in hydrophilicity of the PA, PA/CS, and PA/CS/

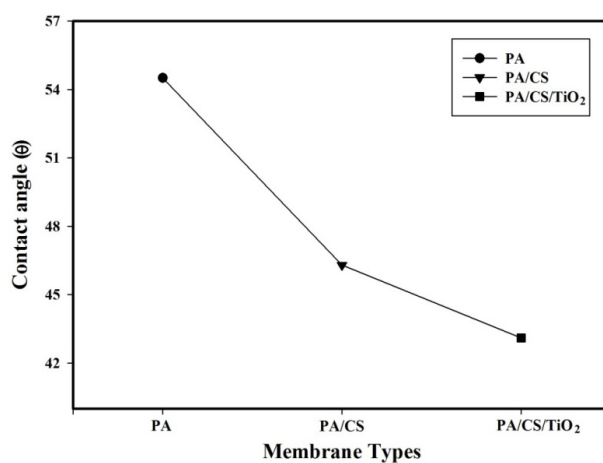


Fig. 11. The contact angle estimation of PA, PA/CS, and PA/CS/TiO<sub>2</sub> modified membranes.

TiO<sub>2</sub> modified membranes. From Fig. 11, PA membrane demonstrates contact angle equals to 54.5° this indicates weak membrane surface wettability with water and moderately hydrophobic. After modification of PA membranes by irradiated chitosan and chitosan/TiO<sub>2</sub> the hydrophilicity of TFC membrane was enhanced, and it diminished to 46.3° and 43.1° respectively. Thus, the modified membranes hydrophilicity increases as a result of chitosan/TiO<sub>2</sub> treatments due to the hydrophilic nature of chitosan and TiO<sub>2</sub>.

## 4. Conclusion

Energy consumption for reverse osmosis can be decreased by making a very high permeability reverse osmosis membrane and putting it to use. The thin-film composite RO membrane can be modified to form a very high-flux membrane by successive chemical treatment with chitosan and a mixture of chitosan/TiO<sub>2</sub> to make the hydrophilic supramolecular assembly. Such a composite membrane demonstrated the lower contact angle and higher hydrophilicity. The water flux and salt rejection were greatly affected by the concentration of chitosan, TiO<sub>2</sub>, and salinity of the medium. The best conditions fulfilled the suitable water flux and salt rejection were 0.2 wt% chitosan, 0.1 wt% TiO<sub>2</sub>, at 10000 ppm salinity NaCl solution.

## Acknowledgements

It is a pleasure to acknowledge the Egyptian Desalination Research Center of Excellence, (EDRC) which follows Desert Research Center, for their supporting to carry out this research.

## References

- [1] L.F. Greenlee, D.F. Lawler, B.D. Freeman, B. Marrot, P. Moulin, Reverse osmosis desalination: water sources, technology, and today's challenges, *Water Res.*, 43 (2009) 2317–2348.
- [2] L. Gongping, W. Wang, J. Wanqin, X. Nanping, Polymer/ceramic composite membranes and their application in pervaporation process, *Chinese J. Chem. Eng.*, 20 (2012) 62–70.

- [3] L. Liu, X. Huang, X. Zhang, K. Li, Y. Ji, C. Yu, C. Gao, Modification of polyamide TFC nanofiltration membrane for improving separation and antifouling properties, *RSC Adv.*, 8 (2018) 15102–15110.
- [4] S. Leong, A. Razmjou, K. Wang, K. Hapgood, X. Zhang, H. Wang, TiO<sub>2</sub> based photocatalytic membranes, a review, *J. Membr. Sci.*, 472 (2014) 167–184.
- [5] J. Kim, B. Van der Bruggen, The use of nanoparticles in polymeric and ceramic membrane structures: review of manufacturing procedures and performance improvement for water treatment, *Environ. Pollut.*, 158 (2010) 2335–2349.
- [6] A.W. Mohammad, Y.H. Teow, W.L. Ang, Y.T. Chung, D.L. Oatley-Radcliffe, N. Hilal, Nanofiltration membranes review: recent advances and future prospects, *Desalination*, 356 (2015) 226–254.
- [7] A.F. Ismail, M. Padaki, N. Hilal, T. Matsuura, W.J. Lau, Thin film composite membrane recent development and future potential, *Desalination*, 356 (2015) 140–148.
- [8] A.G. Fane, R. Wang, M.X. Hu, Synthetic membranes for water purification: status and future, *Angew. Chem. Int. Ed. Engl.*, 54 (2015) 3368–3386.
- [9] L.F. Greenlee, D.F. Lawler, B.D. Freeman, B. Marrot, P. Moulin, Reverse osmosis desalination: water sources, technology, and today's challenges, *Water Res.*, 43 (2009) 2317–2348.
- [10] D. Li, H.T. Wang, Recent developments in reverse osmosis desalination membranes, *J. Mater. Chem.*, 20 (2010) 4551–4566.
- [11] G.M. Geise, D.R. Paul, B.D. Freeman, Fundamental water and salt transport properties of polymeric materials, *Prog. Polym. Sci.*, 39 (2014) 1–24.
- [12] L. Ni, J. Meng, G.M. Geise, Y. Zhang, J. Zhou, Water and salt transport properties of zwitterionic polymers film, *J. Membr. Sci.*, 491 (2015) 73–81.
- [13] C.Y. Tang, Y.N. Kwon, J.O. Leckie, Probing the nano- and micro-scales of reverse osmosis membranes - a comprehensive characterization of physiochemical properties of uncoated and coated membranes by XPS, TEM, ATR-FTIR, and streaming potential measures, *J. Membr. Sci.*, 287 (2007) 146–156.
- [14] K. Li, L. Liu, H. Wu, S. Li, C. Yu, Y. Zhou, W. Huang, D. Yan, Understanding the temperature effect on transport dynamics and structures in polyamide reverse osmosis system via molecular dynamics simulations, *Phys. Chem. Chem. Phys.*, 20 (2018) 29996–30005.
- [15] R. Rangarajan, N.V. Desai, S.L. Daga, S.V. Joshi, A. PrakashRao, V.J. Shah, J.J. Trivedi, C.V. Devmurari, K. Singh, P.S. Bapat, H.D. Raval, S.K. Jewrajka, N.K. Saha, A. Bhattacharya, P.S. Singh, Ray Paramita, G.S. Trivedi, N. Pathak, A.V.R. Reddy, Thin film composite reverse osmosis membrane development and scale up at CSMCRL, Bhavnagar, *Desalination*, 282 (2011) 68–77.
- [16] X.S. Peng, J. Jin, Y. Nakamura, T. Ohno, L. Ichinose, Ultrafast permeation of water through protein-based membranes, *Nat. Nanotechnol.*, 4 (2009) 353–357.
- [17] Y. Li, T.S. Chung, S. Kulprathipanja, Novel Ag<sup>+</sup>-zeolite/polymer mixed matrix membranes with a high CO<sub>2</sub>/CH<sub>4</sub> selectivity, *AIChE J.*, 53 (2007) 610–616.
- [18] T. Tsuru, Inorganic porous membranes for liquid phase separation, *Sep. Purif. Meth.*, 30 (2001) 191–220.
- [19] B.D. Freeman, Basis of permeability/selectivity tradeoff relations in polymeric gas separation membranes, *Macromolecules*, 32 (1999) 375–380.
- [20] M.L. Lind, D.E. Suk, T. Nguyen, E.M.V. Hoek, Tailoring the structure of thin-film nanocomposite membranes to achieve seawater RO membrane performance, *Environ. Sci. Technol.*, 44 (2010) 8230–8235.
- [21] E.M. Vrijenhoek, S. Hong, M. Elimelech, Influence of membrane surface properties on initial rate of colloidal fouling of reverse osmosis and nanofiltration membranes, *J. Membr. Sci.*, 188 (2001) 115–128.
- [22] C.Y. Tang, Q.S. Fu, C.S. Criddle, J.O. Leckie, Effect of flux (transmembrane pressure) and membrane properties on fouling and rejection of reverse osmosis and nanofiltration membranes treating perfluorooctane sulfonate containing wastewater, *Environ. Sci. Technol.*, 41 (2007) 2008–2014.
- [23] G. Alagumuthu, T. Anantha Kumar, Synthesis and characterization of chitosan/TiO<sub>2</sub> nanocomposites using liquid phase deposition technique, *Int. J. Nanosci. Nanotechnol.*, 4 (2013) 105–111.
- [24] Z. Liu, R. Wang, F. Kan, F. Jiang, Synthesis and characterization of TiO<sub>2</sub> nanoparticles, *Asian J. Chem.*, 26 (2014) 655–659.
- [25] F. Rahmawati, I. Fadillah, M. Mudjijono, Composite of nano-TiO<sub>2</sub> with cellulose acetate membrane from nata de coco (nano-TiO<sub>2</sub>/CA(NDC)) for methyl orange degradation, *J. Mater. Environ. Sci.*, 8 (2017) 287–297.
- [26] H. Deng, Y. Xu, B. Zhu, X. Wei, F. Liu, Z. Cui, Polyelectrolyte membranes prepared by dynamic self-assembly of poly(4-styrenesulfonic acid-co-maleic acid) sodium salt (PSSMA) for nanofiltration (I), *J. Membr. Sci.*, 323 (2008) 125–133.
- [27] S.S. Shenvi, S.A. Rashid, A.F. Ismail, M.A. Kassim, A.M. Isloor, Preparation and characterization of PPEES/chitosan composite nanofiltration membrane, *Desalination*, 315 (2013) 135–141.